

Monitoring the ADP/ATP ratio via induced circularly-polarised europium luminescence

Sergey Shuvaev,^[a] Mark A. Fox,^[a] and David Parker^{*[a]}

Abstract: A series of three europium complexes is reported bearing picolyl amine moieties that possess differing binding affinities towards Zn^{2+} and three nucleotides – AMP, ADP and ATP. A large increase of the total emission intensity was observed upon binding Zn^{2+} , followed by signal amplification upon addition of nucleotides. The resulting adducts possess strong induced circularly polarised emission, with ADP and ATP signals being of opposite sign. Model DFT geometries of the adducts suggest the Δ diastereoisomer is preferred for ATP and the Λ isomer for ADP/AMP. Such a change in sign allows the ADP/ATP (or AMP/ATP) ratio to be assessed by monitoring changes in the emission dissymmetry factor, g_{em} .

Adenosine phosphates play an essential role in energy storage at the cellular level.^[1] Monitoring their levels *in cellulo* is of particular importance for getting a deeper insight into many biological processes. For instance, the ratio between ATP molecules released from mitochondria and ADP molecules trapped from the cytosol into the matrix, mediated by ADP/ATP translocase, may indicate the presence of severe pathologies, such as mitochondrial myopathies.^[2] One of very few known examples of a ratiometric luminescence probe to monitor the ADP/ATP ratio is the fusion protein Perceval, consisting of a bacterial regulatory protein GlnK1 and a modified green fluorescent protein GFP.^[3] A more recent example of a luminescent probe capable of monitoring the ADP/ATP ratio based on small molecules was reported by Butler, where a europium complex with a DO2A-based ligand bearing two quinolone-derived chromophores stabilises nucleotide molecules via hydrogen bonding.^[4]

Europium complexes have been used extensively for selective anion binding, often generating a ratiometric response in emission.^{[5],[6]} Different strategies to modulate selectivity and binding affinities have been employed, including steric complementarity,^[7] variation of the overall charge^[8] and introduction of stabilising and orienting weak interactions, such as hydrogen bonding,^[9] π - π stacking,^[10] or boron-carbohydrate interactions.^[11] Furthermore, the high rotatory strength^[12] of certain magnetic-dipole allowed transitions in Eu^{3+} complexes can give rise to a strong circularly-polarised luminescence (CPL) signal, with a dissymmetry factor (g_{em}) of up to 1.4. Such g_{em} values are about two orders of magnitude higher than in organic

molecules or transition metal complexes. In comparison with circular dichroism (CD) spectroscopy, CPL spectroscopy provides higher sensitivity, whilst its ability to resolve transitions otherwise invisible in conventional luminescence spectroscopy renders it advantageous over total emission spectral analysis. Strong CPL signals of europium and terbium complexes have been exploited to create pH,^[13] temperature,^[14] protein^{[15],[16],[17],[18]} and anion-sensitive^{[19],[20],[21],[22]} CPL probes, whose dissymmetry factor has been monitored as a function of pH or added analyte. Deviations in cellular uptake of different enantiomers can also be exploited, with the advent of chiral luminescence microscopy, by detecting the CPL signal from enantiomeric complexes *in cellulo*.^[23]

Adenosine phosphates are naturally chiral anions, and they can give rise to a signal that can be detected by chiroptical methods. It has been shown, for example, that ADP and ATP may produce signals of opposite handedness once they are added to a zinc complex by forming a helical oligomer.^{[24],[25]} CD spectroscopy was used to monitor the ratio between ADP and ATP molecules in the solution; such an approach is not applicable *in cellulo*.

With this background in mind, a series of DO2A-based complexes $[EuL^{1-3}]$ bearing an alkynyl-pyridine chromophore and a substituted picolylamine moiety has been synthesised, whose bimetallic Zn^{2+} complexes $[EuL^1]_2 \cdot Zn^{2+}$ and $[EuL^2]_2 \cdot Zn^{2+}$ showed CPL spectra of opposite handedness when ADP and ATP were added. Moreover, subtle structural changes in the ligand design significantly modulated the binding affinities of $[EuL^{1-3}]$ towards Zn^{2+} and nucleotides.

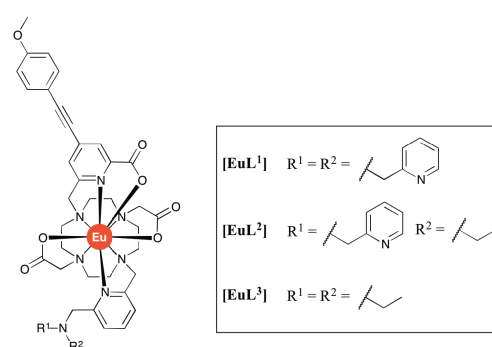


Figure 1 Molecular structures of $[EuL^{1-3}]$

Each complex $[EuL^{1-3}]$ was synthesised by successive alkylation reactions of a DO2A-ethyl ester precursor, followed by basic hydrolysis and complexation with $EuCl_3 \cdot 6H_2O$ (see ESI for synthetic details). The picolylamine moiety bore dipicolyl ($[EuL^1]$), ethylpicolyl ($[EuL^2]$) or diethyl ($[EuL^3]$) substituents, giving a gradually decreasing number of hydrogen bond acceptors, i.e. tertiary amine and pyridine nitrogen atoms.

[a] Prof..Dr. David Parker
Dr. Sergey Shuvaev, Dr. Mark A. Fox
Department of Chemistry
Durham University
South Road Durham DH1 3LE (United Kingdom)
E-mail: sergey.shuvaev@durham.ac.uk
david.parker@durham.ac.uk

Supporting information for this article is given via a link at the end of the document.

The parent complex, **[EuL¹]**, inspired by a related system first reported by Pope^[26], showed a high affinity ($\log K = \log K_1K_2 \sim 12.7$) towards Zn^{2+} with a 1:2 binding stoichiometry (Figs. S1, S2 and S31). Zinc complexation was accompanied by a 4-fold increase of the total emission intensity and changes in the spectral signature, upon excitation at 335 nm (Fig. S1). Significant changes in the number and relative intensities of the Stark splitting components suggest dissociation of the pyridine nitrogen *trans* to the chromophore, which is instead bound to Zn^{2+} . The concomitant increase in metal hydration number, q , suggests the stabilisation of additional water molecules, presumably via hydrogen bonding to the pyridine nitrogen atoms and the Zn^{2+} ion. In similar binding experiments with Ca^{2+} and Mg^{2+} , only minor changes of the total emission intensity were detected, with no changes of the spectral signature. At the same time, addition of Cu^{2+} and Ni^{2+} considerably quenched the emission intensity of Eu^{3+} via a photoinduced electron transfer process. However, these ions are present in a free form at significantly lower concentrations *in cellulo* compared to Zn^{2+} .

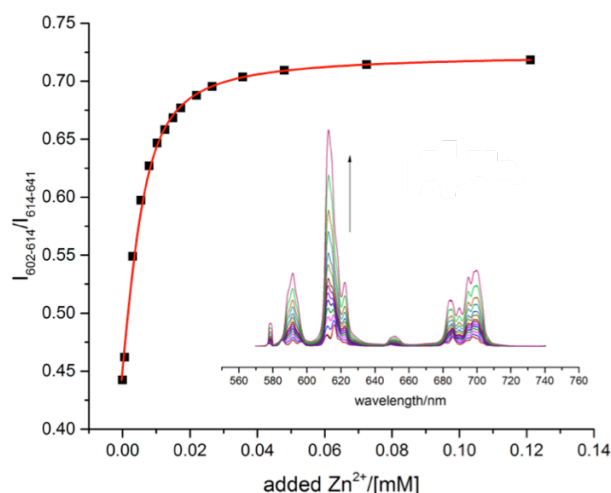


Figure 2 Variation of the europium emission spectrum upon binding Zn^{2+} to **[EuL²]** (**[EuL²]** 8 μ M, 0.1 M HEPES, pH = 7.40, 298K, λ_{ex} = 335 nm). The binding affinity ($\log K = 5.6(0.1)$) was fitted assuming 1:1 binding.

The complex, **[EuL²]**, with only one picolyl group, showed a lower affinity towards Zn^{2+} ($\log K = 5.6(0.1)$) (Fig. 2). The emission spectrum showed large changes in form and a 7-fold rise in intensity, whilst the lifetime of the excited state almost doubled ($\tau = 0.46$ ms vs $\tau = 0.24$ ms, Fig. S3). Like **[EuL¹]**, the hydration number, q , increased by one following addition of zinc. The Job plot showed an intersection of two straight lines at molar fraction of $Zn^{2+} \times = 0.5$, corresponding to 1:1 binding stoichiometry (Fig. S4). However, these ratios obtained using a Job plot analysis should be treated with care, as limitations in determining stoichiometry in supramolecular systems have been demonstrated.^[27]

In contrast to **[EuL¹]** and **[EuL²]**, the complex **[EuL³]** showed no significant changes in the emission, following addition of Zn^{2+} . The emission intensity signature of **[EuL³]** was modulated as a function of pH with an apparent pK_a of 8.4 (0.1), ascribed to reversible protonation of the tertiary aliphatic amine (Fig. S25).

Similar behaviour was observed with **[EuL¹]** and **[EuL²]**, where the spectral signature changed upon varying pH from 7.4 up to 10, indicating that protonation of the tertiary amine takes place in each case under the experimental conditions used for nucleotide binding (0.1 M HEPES, pH = 7.4).

Table 1 Apparent binding constants ($\log K_a$) fitted in 1:1 and 1:2 binding model in H_2O for **[EuL¹]** and **[EuL²]** upon addition of Zn^{2+} and Zn^{2+} with nucleotides.

Complex ^a	Zn^{2+}	Zn^{2+} +AMP	Zn^{2+} +ADP	Zn^{2+} +ATP
[EuL¹]	12.7 ^b	4.5(0.1)	4.8(0.1)	4.7(0.1)
[EuL²]	5.6(0.1)	4.2(0.1)	5.5(0.1)	4.6(0.1)

a) **[EuL¹]** showed no significant affinity for Zn^{2+} , and only very low binding constants were estimated upon addition of nucleotides; b) Fitted using a 1:2 model

Table 2 Lifetimes (ms) in H_2O and hydration numbers (q) in parentheses for **[EuL¹]** and **[EuL²]** following addition of Zn^{2+} and nucleotides (0.15 mM).

Complex	water	Zn^{2+}	AMP	ADP	ATP
[EuL¹]	0.54 (0.4)	0.45 (1.4)	0.97 (0)	0.99 (0)	0.97 (0)
[EuL²]	0.24 (0.6)	0.47 (1.3)	1.09 (0)	1.09 (0)	1.10 (0)

Complexes **[EuL¹⁻²]** experienced considerable changes in their emission spectra and excited state lifetimes upon binding of the nucleotides AMP, ADP and ATP. Relatively high binding affinities ($\log K > 6$) were observed for **[EuL¹]**, with a somewhat lower affinity detected upon addition of ATP (Fig. S5). The biggest spectral changes were observed with AMP (defined as the ratio $I_{602nm-614nm}/I_{614nm-641nm}$, Fig. S6), followed by ATP and ADP (Fig. S7). The total emission intensity experienced a 7-, 4- and 11-fold increase upon addition of AMP, ADP and ATP, respectively. In the case of **[EuL²]** almost three orders of magnitude lower binding affinities were observed for each nucleotide (Fig. S9), whilst the biggest spectral change ($I_{602nm-614nm}/I_{614nm-641nm}$) was observed upon addition of AMP, followed by ADP and ATP, respectively (Fig. S10). The enhancement of the total emission intensity followed the same trend, being biggest for AMP (8-fold), intermediate for ADP (4-fold) and lowest for ATP (no change). Excitation spectra experienced only minor changes upon addition of nucleotides to **[EuL²]** (Fig. S23). Different binding affinities of each nucleotide were observed for the systems with added Zn^{2+} ions (Figs. S17-S22). In the case of **[EuL¹]**, we assumed that the initial 1:2 complex **[EuL¹]₂Zn²⁺** partially dissociates forming a 1:1 species **[EuL¹]⁺Zn²⁺** in the presence of excess zinc, which then binds a nucleotide. Remarkable increases in the total emission intensity and lifetime were observed after addition of AMP, ADP and ATP (Figs. S13, S14). Furthermore, a noticeable change in the position of the Stark components of the $^5D_0 \rightarrow ^7F_4$ transition was observed; this spectral change was used to follow complexation and permit binding analysis. For each nucleotide, a $\log K$ value of $\sim 4-5$ was

observed, consistent with a structure for $[\text{EuL}^1]\cdot\text{Zn}^{2+}$ with pyridine nitrogen atoms that are involved in zinc binding instead of nucleotide binding, as the log K value is lower than for the $[\text{EuL}^1]$ complex with each nucleotide. The water molecule bound to the europium centre was replaced by a phosphate oxygen in each case ($q = 0$), whilst the total emission intensity experienced a 2 to 3 fold increase. A similar increase of the total emission intensity was observed for $[\text{EuL}^2]\cdot\text{Zn}^{2+}$ upon addition of AMP (3-fold), ADP (2-fold) and ATP (no change) (Figs. S15, S16). The significant decrease of binding affinities from $[\text{EuL}^1]$ to $[\text{EuL}^3]$ following replacement of the picolyl moieties with an ethyl group, highlights the key role of the pyridine groups. Thus, the removal of both picolyl moieties in $[\text{EuL}^3]$, resulted in very low binding constants, with no saturation values reached at concentrations close to maximum solubilities of added nucleotides. This effect is even more important with added zinc, where the pyridine groups offer a well-defined binding site for the metal ion, with the exocyclic pyCH_2N sub-unit offering two more donors, following dissociation from Eu and deprotonation of the tertiary amine nitrogen atom.

It is hypothesised that in the absence of zinc, a hydrogen bond between one phosphate oxygen of the nucleotide and the protonated tertiary amine N plays a key role in stabilising the bound species. In the presence of zinc, this proton is lost, and the exocyclic ligand nitrogen atoms coordinate zinc; the bound zinc then can become 5-coordinate by bridging to the phosphate that is coordinated to europium, stabilizing and rigidifying this ternary adduct.

Experimental evidence to assess the involvement of a π - π stacking interaction between the pyridine ring of the complex and the adenine heterocycle was considered. Addition of HPO_4^{2-} (i.e. where no π - π stacking is possible) showed binding affinities similar to those obtained upon addition of nucleotides (Figs. S11, S12). Thus, whilst a weak π - π interaction cannot be ruled out (e.g. some changes are visible in the excitation spectrum of $[\text{EuL}^2]\cdot\text{Zn}$ upon addition of ADP, Fig. S24), the free energy contribution stabilising the bound species is less significant than electrostatic, H-bonding and hydrophobic interactions.

DFT simulations were carried out on model geometries of complexes explored here (see ESI for computational details, Figures S26-S37) to help rationalise the experimental behaviour. These calculations confirmed that there was no significant coplanar overlap between the nitrogenous base and any of the pyridine rings. Model geometries for the zinc adducts of $[\text{EuL}^1]$ with AMP, ADP and ATP revealed that the terminal phosphate group can bridge the Eu^{3+} and Zn^{2+} ions, thereby stabilising the structures, as visualised for the ADP and ATP adducts in Figures 3, S34 and S35.

The most striking spectral observation was discovered upon recording the CPL spectra of $[\text{EuL}^1]_2\cdot\text{Zn}^{2+}$ aggregates with bound nucleotide (Fig. S8). Each complex revealed a relatively intense CPL signal at $\lambda = 592$ nm, with ATP and ADP having a negative dissymmetry factor g_{em} value ($g_{\text{em}} = -0.070$ for added AMP and $g_{\text{em}} = -0.032$ for added ADP, respectively), whilst ATP showed a positive g_{em} ($g_{\text{em}} = +0.042$). The highest $|g_{\text{em}}|$ value for added AMP is in line with the shorter distance between Eu^{3+}

and the chiral sugar moiety which is supported by DFT data (Figure S33).

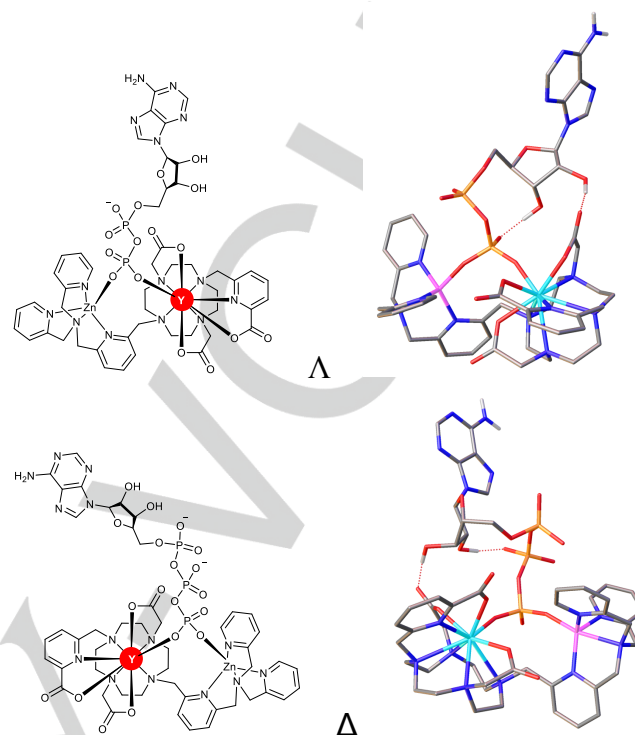
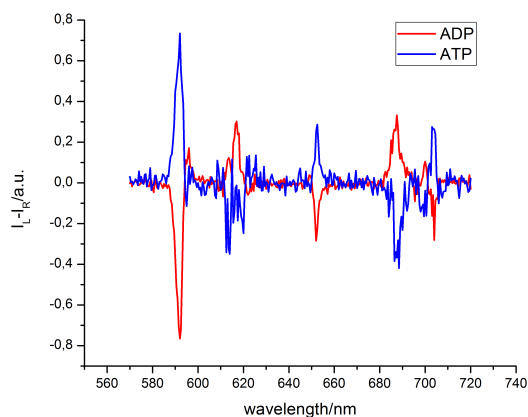


Figure 3 Optimised model geometries for $[\text{EuL}^1]\cdot\text{Zn}^{2+}\cdot\text{ADP}$ (upper) and $[\text{EuL}^1]\cdot\text{Zn}^{2+}\cdot\text{ATP}$ (lower) showing different arrangements of the exocyclic ring substituents (Λ / Δ); Y is used as a surrogate for Eu. Hydrogen atoms are omitted for clarity except at oxygen and nitrogen atoms. The dotted bonds show hydrogen bond interactions. The structures of the higher energy diastereoisomers are given in the ESI.

The opposite signs of the CPL spectra for the ADP and ATP adducts suggest a preference for different conformers, as shown in Figure 3, where the Λ form is more stable in the ADP (and AMP) adduct, whereas the Δ form is preferred energetically in the ATP adduct (Figs. S34 and S35).

Similar findings were observed for $[\text{EuL}^2]\cdot\text{Zn}^{2+}$ following addition of each nucleotide. The total emission intensity rose four- and two-fold upon addition of AMP and ADP respectively, with the spectral signature and the lifetime experienced a considerable change in each case. The binding constant was the highest for added ADP (log K = 5.5) and lowest for AMP (log K = 4.2), whilst CPL spectra of opposite signs were recorded for $[\text{EuL}^2]\cdot\text{Zn}^{2+}$ with added AMP/ADP and ATP (Fig. 4). A higher emission dissymmetry factor was recorded upon addition of ADP ($g_{\text{em}} = -0.038$), which was lower for both AMP and ATP ($|g_{\text{em}}| = 0.009$ for each). Given that these g_{em} values do not follow the expected trend with an increasing distance between europium and the chiral sugar moiety, as well as opposite signs of induced CPL spectra were observed for AMP/ADP and ATP, there must be increased flexibility with the nucleotide molecule due to the absence of a picolyl group in L^2 compared to L^1 . A more detailed inspection of the high-resolution emission spectra supports this conclusion, as noticeable changes were observed between the AMP and ADP/ATP adducts (Fig. S9). Even though the luminescence spectra were identical for the ADP and ATP

adducts, the opposite signs of their CPL spectra indicate that different orientations of a sugar moiety do not perturb the primary coordination environment at Eu^{3+} and produced identical emission spectra.



The sign

Figure 4 CPL spectra of $[\text{EuL}_2]^+\text{Zn}^{2+}$ with added ADP and ATP ($[\text{EuL}_2]^+$ 5 μM , ZnCl_2 60 μM , 0.1 M HEPES, pH = 7.40, 298 K, λ_{ex} = 335 nm), showing their opposite handedness.

inversion of g_{em} for the ADP and ATP adducts allow their ratio in a mixture to be assessed from their CPL spectra, as the resulting dissymmetry factor does not depend on the concentration of individual components, once the concentration of each nucleotide is above the threshold value, i.e. when the binding curve reaches a plateau. The g_{em} value was followed as a function of the ratio between ADP and ATP species varying from $[\text{EuL}_2]^+\text{Zn}^{2+}\text{ADP}$ ($g_{\text{em}} = -0.038$) to $[\text{EuL}_2]^+\text{Zn}^{2+}\text{ATP}$ ($g_{\text{em}} = 0.009$) (Fig. 5). The total concentration of the two nucleotides was kept constant (0.1 mM), which in each case approximately corresponded to the onset of the binding plateau. A gradual increase of the $-g_{\text{em}}$ value was observed upon increasing the ATP/ADP ratio, consistent with the opposite signs in their CPL.

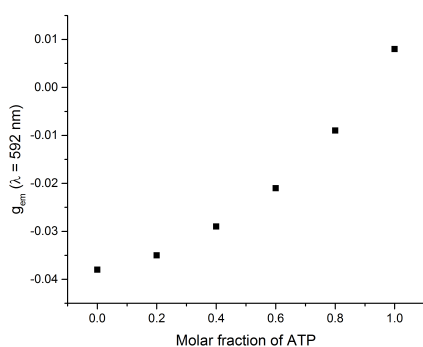


Figure 5 Variation of $-g_{\text{em}}$ ($\lambda = 592$ nm) as a function of the ADP/ATP ratio for $[\text{EuL}_2]^+\text{Zn}^{2+}$ at constant total concentration of nucleotides ($[\text{EuL}_2]^+$ 10 μM , ZnCl_2 100 μM , 0.1 M HEPES, ADP+ATP 0.1 mM, pH = 7.40, 298K, λ_{ex} = 335 nm).

In summary, for the first time, an induced CPL signal can be used to distinguish the binding of nucleotides and can enable the monitoring of the ratio between ADP and ATP directly in solution. Different binding modes of these nucleotides to $[\text{EuL}_1]^+\text{Zn}^{2+}$ and $[\text{EuL}_2]^+\text{Zn}^{2+}$ result in the opposite handedness of their induced CPL spectra, allowing their ratio to be monitored at

sub-millimolar/millimolar levels by following the variation of the dissymmetry ratio, g_{em} .

Acknowledgements We thank Durham University for a Doctoral Scholarship (S.S.). The authors would like to thank Dr. Ilya Zlotnik for his help with fitting binding curves.

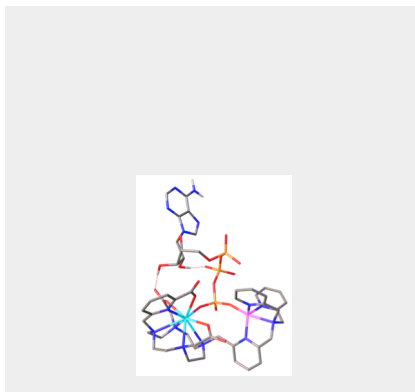
Keywords: Europium • CPL • ADP • ATP • Luminescence

- [1] T. Hunter, *Philos. Trans. R. Soc. B Biol. Sci.* **2012**, 367, 2513–2516.
- [2] M. Milone, L.-J. Wang, *Mol. Genetics Metabolism*, 2013, **111**, 35–41.
- [3] J. Berg, Y. P. Hung, G. Yellen, *Nat. Methods* **2009**, 6, 161–166.
- [4] S. H. Hewitt, J. Parris, R. Mailhot, S. J. Butler, *Chem. Comm.* **2017**, 53, 12626–12629.
- [5] S. J. Butler, D. Parker, *Chem. Soc. Rev.* **2013**, 42, 1652–1666.
- [6] S. Shuvaev, M. Starck, D. Parker, *Chem. - Eur. J.* **2017**, 23, 9974–9989.
- [7] J. Sahoo, R. Arunachalam, P. S. Subramanian, E. Suresh, A. Valkonen, K. Rissanen, M. Albrecht, *Angew. Chem. - Int. Ed.* **2016**, 55, 9625–9629.
- [8] R. Pal, D. Parker, L. C. Costello, *Org. Biomol. Chem.* **2009**, 7, 1525–8.
- [9] S. J. Butler, *Chem. Commun.* **2015**, 51, 10879–10882.
- [10] E. Weitz, J. Y. Chang, A. H. Rosenfield, E. Morrow, V. C. Pierre, *Chem. Sci.* **2013**, 4, 4052.
- [11] E. R. Neil, D. Parker, *RSC Adv.* **2017**, 7, 4531–4540.
- [12] F. Zinna, L. Di Bari, *Chirality* **2015**, 27, 1–13.
- [13] D. G. Smith, B. K. McMahon, R. Pal, D. Parker, *Chem. Comm.* **2012**, 48, 8520.
- [14] J. Yuasa, H. Ueno, T. Kawai, *Chem. - Eur. J.* **2014**, 20, 8621–8627.
- [15] C. P. Montgomery, E. J. New, D. Parker, R. D. Peacock, *Chem. Comm.* **2008**, 4261–4263.
- [16] J. Yuasa, T. Ohno, H. Tsumatori, R. Shiba, H. Kamikubo, M. Kataoka, Y. Hasegawa, T. Kawai, *Chem. Comm.* **2013**, 49, 4604.
- [17] L. Jennings, R. S. Waters, R. Pal, D. Parker, *ChemMedChem* **2017**, 12, 271–277.
- [18] S. Shuvaev, R. Pal, D. Parker, *Chem. Comm.* **2017**, 53, 6724–6727.
- [19] C. Noguez, F. Hildalgo, *Chirality* **2014**, 26, 553–562.
- [20] E. R. Neil, M. A. Fox, R. Pal, L. O. Palsson, B. O'Sullivan, D. Parker, *Dalton Trans.* **2015**, 44, 14937–14951.
- [21] E. R. Neil, M. A. Fox, R. Pal, D. Parker, *Dalton Trans.* **2016**, 45, 8355–8366.
- [22] K. Okutani, K. Nozaki, M. Iwamura, *Inorg. Chem.* **2014**, 53, 5527–5537.
- [23] A. T. Frawley, R. Pal, D. Parker, *Chem. Comm.* **2016**, 52, 13349–13352.
- [24] M. Kumar, P. Brocorens, C. Tonnelé, D. Beljonne, M. Surin, S. J. George, *Nature Comm.* **2014**, 5, 5793.
- [25] M. Kumar, N. Jonnalagadda, S. J. George, *Chem. Comm.* **2012**, 48, 10948.
- [26] S. J. A. Pope, R. H. Laye, *Dalton Trans.* **2006**, 44, 3108–3113.
- [27] F. Ulatowski, K. Dabrowa, T. Bałakier, J. Jurczak, *J. Org. Chem.* **2016**, 81, 1746–1756.

Entry for the Table of Contents (Please choose one layout)

COMMUNICATION

Circularly polarised luminescence signals the inversion in metal complex helicity occurring when binding ADP vs ATP



*Sergey Shuvaev, Mark A Fox, David Parker**

Page xxx -xxxx

Monitoring the ADP/ATP ratio via induced circularly-polarised europium luminescence
